Asymmetric Illumination Contrast: A Method of Image Formation for Video Light Microscopy

Abstract. *Images with high resolution and exceptionally broad gray scale can be obtained by the application of video contrast enhancement to an optimized procedure for imaging transparent objects with oblique rays of illumination. This technique is simple to set up. A conventional microscope with a light source whose position can be adjusted and a video camera with controls for gain and black level are the only essential components. Features such as high resolution, optical sectioning, control of contrast, and operation under low light intensity make this technique preferable, in several instances, to currently used video microscopy techniques.*

That oblique rays of illumination can generate image contrast has been known empirically since the end of the 19th century. However, because this phenomenon was not well understood at that time, and because of the intrinsic defects of the early methods, the early attempts to obtain quality images of transparent objects with oblique illumination were unsuccessful (*1, 2*). With the advent of phase-contrast microscopy (*3, 4*) such methods were in general abandoned. Modulation contrast (*5*) and single sideband edge enhancement (*1*) are two current techniques that take advantage of oblique rays to produce useful images and reduce the disadvantages of the early procedures. But because of the required use of slit appertures and half stops in the light path, some limitations and artifacts still remain (*2, 6*). Recently, video technology has been applied to overcome limitations in many light microscopy techniques (*7–10*), particularly as a means to enhance contrast in differential interference contrast (DIC) microscopy (*8, 9*). I now describe an alternative video microscopy procedure that makes use of oblique rays of illumination, is simple to set up, and has several advantages over video-enhanced DIC.

Transparent objects, when illuminated with parallel rays of light, do not produce visible images in ordinary bright-field microscopy because the sum of the diffracted light, from each detail of the object focused by the objective lens at the image plane (Fig. 1a), is 1/4 wave out of phase with the direct light (*1, 3, 4, 11*). It can be demonstrated, however, that for each point in the specimen, each side of the lateral components of the diffracted light (a "sideband") is offset from the 1/4 wave displacement in an equal and opposite way (*1, 3*). Consequently, if one sideband of the diffracted light from the object is prevented from reaching the image plane, constructive and destructive interference will occur between the remaining sideband and the direct light to produce a visible image at the plane of focus (*1, 3*). Suppression of a sideband from the image formation process can be obtained for oblique rays of illumination.

When a bright-field microscope is operated at high numerical aperture and in Kohler illumination, the most oblique rays of the illuminating cone produce diffracted light, which is scattered such that up to one sideband is outside of, and thus excluded from, the objective apperture (Fig. 1, b and c). Under normal operating conditions, no visible image is produced because the illumination is symmetrical. Symmetric oblique rays produce complementary patterns of diffracted light such that, in the end, no significant constructive or destructive interference with the direct light occurs at the image plane. By making the intensity of light in the cone of illumination uneven (asymmetric illumination) this balance is offset. A visible image results with the difference of intensity between interference patterns of the diffracted light from opposing oblique rays of the asymmetric illuminating cone.

To obtain asymmetric illumination, the lamp filament is simply displaced from the optical axis (Fig. 2a). With the filament offset, the regular diffuser glass in front of the lamp spreads the light to fill the condenser aperture with a gradient of illumination (Fig. 2b). This gradient provides the requisite imbalance of oblique rays.

The images obtained by this method, hereafter referred to as asymmetric illumination contrast (AIC), appear shadowed, similar to images obtained by DIC microscopy (*12*) or other shadow-casting techniques (*1, 5*). With AIC, the direction of shadow in the image is parallel to the direction of the gradient of light intensity (Fig. 2b) of the asymmetric illuminating cone. Phase-advancing details are shadowed in the direction opposite to that of phase-retarding details.

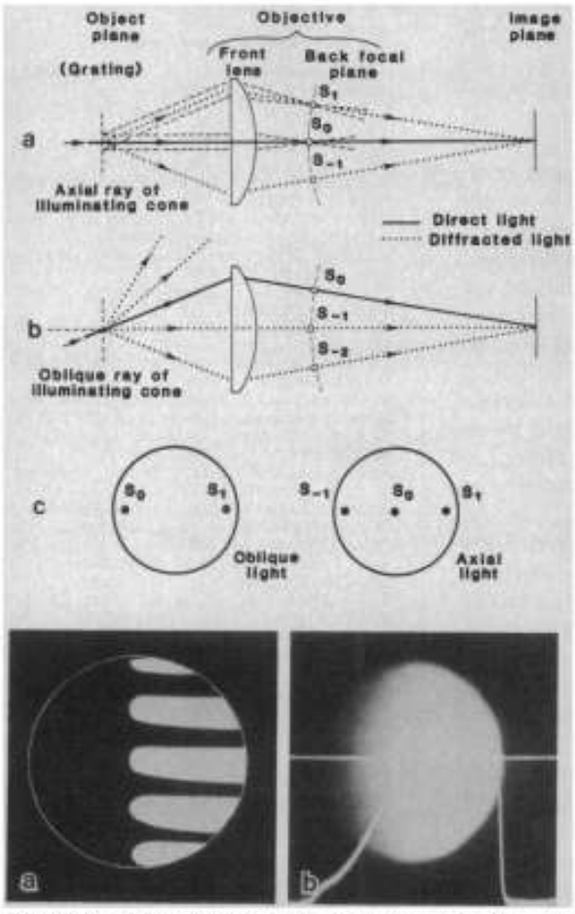

Fig. 1 (top). Diffracted light entering an objective originating from parallel (axial) (a) or oblique (b) rays of illumination when the specimen is a diffraction grating. With axial rays of illumination, symmetrical components of the diffracted light are admitted by the objective; with oblique illumination, one side of the lateral components of diffracted light are not taken in by the objective. With oblique rays of illumination, additional single side lateral components of diffracted light may be admitted, enhancing the correspondence between the image formed and the object (*4*). Since only two neighboring diffraction maxima at the posterior focal plane of the objective (c) are necessary for image formation, oblique light will produce a periodic illumination in the image plane when the grating is only half that of the one resolved with normal light (*3, 4*). Fig. 2 (bottom). Image of the laterally displaced tungsten filament of the illuminating bulb (a) focused at the condenser iris in the absence of the diffuser glass. In (b) an intensity trace shows the gradient of light along the horizontal line obtained after replacing the diffuser glass. In most cases, placement of the filament image to cover half of the condenser diaphragm produces the optimum gray tones. However, slight displacement from this position, as well as use of different diffuser glasses, may also contribute to modulation of image contrast.

Images with complementary shadows are obtained when the lamp filament is displaced in an opposite, symmetric direction in relation to the optical axis.

AIC depends on having the condenser aperature diaphragm wide open to obtain maximum imbalance of illumination and maximum resolution (*3, 4*) from the most oblique rays of the illuminating cone (Fig. 1c). When the condenser aperture diaphragm is wide open, however, the contrast of the image seen directly in the microscope is low because of the large amount of light scattered from regions of the specimen not in the field of view. However, image contrast can be amplified electronically by connecting a television camera to the microscope (*7–10*). Very fine, low-contrast details can be detected, especially if a high resolution camera, equipped with both variable gain and offset (black level) adjustments, is used (*8, 9*).

Video enhancement also allows the less intense rays of the darker side of the condenser to contribute critically to resolution of the final image. These rays provide for the resolution of spatial frequencies perpendicular to the orientation of the asymmetric gradient of the illuminating cone. This is possible because the optical image in AIC has a narrow amplitude of contrast and a broad gray scale allowing extensive video contrast enhancement of the whole image without loss of the low-intensity signals when offset is added to compensate for high video gains.

AIC worked well on a Zeiss Axiomat, Nikon Optiphot, and a Zeiss ICM inverted microscope equipped for a bright-field illumination with standard tungsten filament bulb. The video cameras used were either a Newvicon-Dage 65 (Dage-MTI) or a Chalnicon-Hamamatsu c-1000 (Hamamatsu Systems) equipped with gain and offset adjustments (*13, 14*).

The test objects in Fig. 3, a and b, illustrate the high-resolution shadowcast images obtained (*15*). Figure 3a shows a thin optical section at the surface of a human buccal epithelial cell where the surface ridges can be seen in great detail. For this type of specimen this technique provides equal or better images than the polarized light-based video microscopy (*16*). Images viewed by this technique are not obscured by phase objects above or below the plane of focus (Fig. 3, c and d).

When the general imaging capabilities of video-enhanced AIC are compared with those of video-enhanced DIC to reveal submicroscopic structures in thin (*9*) or isotropic specimens (*17*), DIC produces optimum contrast. However, phase gradients are better resolved with AIC when the specimen contains highly birefringent objects. The amplitude of light intensity generated by DIC images of such specimens cannot always be contained within the dynamic range of currently available television cameras (*14*). Thus, when birefringent structures such as secretory or pigment granules, compact lipid formations, chloroplasts, or crystalline inclusions are present, they produce a glare in the video image that limits the useful expansion of the gain of the camera, preventing the enhancement of contrast and visualization of other structures in the field of view. With AIC, the broad gray scale and narrow variation in light intensity of the optical image permits extensive video enhancement producing undisturbed visualization of fine phase gradients (Fig. 3, e and f).

Since AIC does not require the use of cross polarizers or modulators, it can generate images at much lower light in-

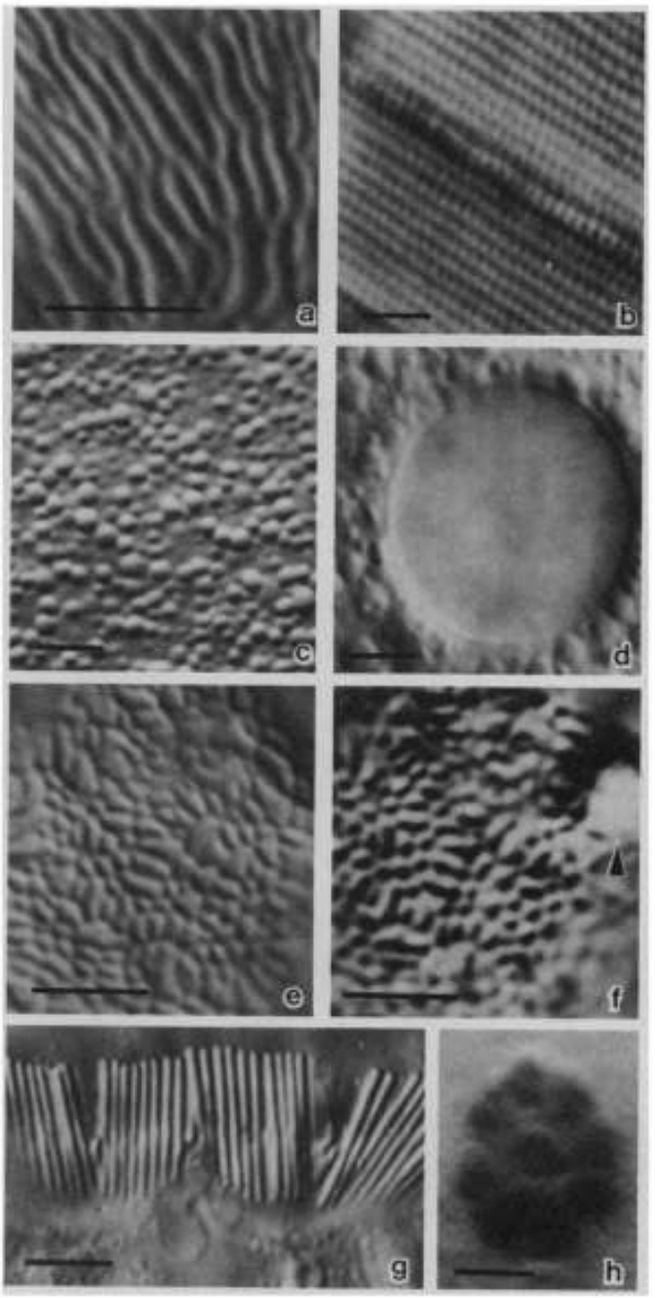

Fig. 3. (a to d) Video-enhanced–asymmetric illumination contrast micrographs of phase objects. Phase variation is converted into intensity variation in the image. The optical shadowing and the three-dimensional appearance results because opposite gradients of phase variation produce opposite gradients of light intensity. The background is adjusted to an adequate gray level by adjusting the gain and black level controls of the camera. In (a), ridges at a portion of the surface of a human buccal epithelial cell are well resolved with a ×100 Planapo objective with a numerical aperture (NA) of 1.3, 1.4-NA oil immersion condenser, and green monochromatic filter. In (b), the lattice structure of the frustule of the diatom *Surirella gemma* (0.41-μm unit repeat) is resolved with a ×40 1.0-NA objective and blue monochromatic illumination. (c and d) The optical sectioning effect in this technique, which corresponds to the cortical and nuclear regions, respectively, of a 100-μm-thick sea urchin egg. The effect by the presence of birefringent structures below or above the plane of focus is illustrated in the equivalent video-enhanced AIC (e) and DIC (f) images of apical surface ridges of cuboidal amphibian kidney (A6) epithelial cells in culture. In the video-enhanced DIC image (f), the presence of a highly birefringent granule below the plane of focus (arrow) degrades the in-focus image of the surface ridges, whereas the VE-AIC image (e) is undisturbed by such structures. (g and h) Optical sections through a whole-mount preparation of guinea pig organ of Corti processed with immunoperoxidase techniques. (g) Stereocilia from the apical region of inner hair cells. (h) A rosette of glutaminase immunoreactive synaptic terminals at the base of one of these cells obtained after changing focus and readjusting the gain and black level controls of the camera. Scale bar, 2.5 μm.

tensity than most techniques, which can be of critical advantage for viewing light-sensitive specimens. This method of image formation does not require any system of rings, slits, or half stops. Therefore, it also avoids halos or diffraction fringes arising from the presence of abrupt edges in the path of illumination (*6*) as in phase-contrast microscopy (*4*). Video-enhanced AIC is also especially suitable for observation of mixed phase and amplitude objects such as cytochemically labeled specimens (Fig. 3, g and h). Weakly labeled structures can easily be seen (Fig. 3h), and clear imaging of any other focal plane in the specimen (Fig. 3g) can be obtained with simple readjustments of the camera's gain and black level.

The video-enhanced AIC technique results from the application of video-derived contrast enhancement to an optimized procedure of imaging transparent objects with oblique rays of illumination. With this combination, images with the highest resolution and exceptionally broad gray scale can be obtained. This technique has several advantages over other video light microscopy techniques and is simple, depending only on minor adjustments to currently available standard equipment. These advantages increase the versatility and range of application of video-enhanced light microscopy to virtually any type of specimen.

BECHARA KACHAR

Laboratory of Neurobiology, National Institute of Neurological and Communicative Disorders and Stroke, National Institutes of Health, Bethesda, Maryland 20205

References and Notes

1. G. Ellis, in *Cell Reproduction*, E. Dirksen, D. M. Prescott, C. E. Fox, Eds. (Academic Press, New York, 1978), pp. 465–476.
2. In the early methods to obtain oblique illumination, such as by racking the iris diaphragm off center, the contrast of the optical image is not notably enhanced until the illumination aperture is reduced to a small zone at one edge of the objective aperture. This procedure compromises resolution, degrades depth discrimination, and introduces a disturbing apparent movement with change in focus.
3. F. Zernike, in *Concepts in Classical Optics*, J. Strong, Ed. (Freeman, San Francisco, 1958), pp. 525–536.
4. M. Francon, *Progress in Microscopy* (Row Peterson, Evanston, Ill., 1962).
5. R. Hoffman and L. Gross, *Nature (London)* **254**, 586 (1975); *Appl. Optics* **14**, 1169 (1975).
6. A diffraction phenomenon of importance in microscopy is the so-called boundary wave, which is observed when light is diffracted by an abrupt edge of a screen or other sharp discontinuity in its path (*4*).
7. J. A. Dvorak, L. H. Miller, W. C. Whitehouse, T. Shiroiski, *Science* **187**, 748 (1975).
8. S. Inoue, *J. Cell Biol.* **89**, 346 (1981).
9. R. D. Allen, N. S. Allen, J. L. Travis, *Cell Motil.* **1**, 291 (1981).
10. R. D. Allen, J. L. Travis, N. S. Allen, H. Yilmaz, *ibid.*, p. 275.
11. F. Zernike, *Science* **121**, 345 (1955).
12. G. Normarski, *J. Phys. Radium* **16**, 9 (1955); R. D. Allen, B. F. David, G. Nomarski, *Z. Wiss. Mikrosk.* **69**, 193 (1969).
13. Under conditions of high video gains, a mottle pattern appears in the image background because of unavoidable dirt and imperfections in the microscope lenses (*14*). A frame memory processor (Hamamatsu Systems, Inc.) is helpful to subtract this pattern continuously from succeeding frames (*14*).
14. R. D. Allen and S. N. Allen, *J. Microsc.* **128**, 193 (1982).
15. The magnification of the images seen on a 19-inch video monitor was ×15,000 and represented an optical section approximately 0.2 μm thick. The video images were recorded on 3/4-inch tapes. Still pictures of the monitor were taken with a Polaroid camera.
16. Compare Fig. 3a to figure 7 in (*8*) and figure 3 in (*9*).
17. S. T. Brady, R. J. Lasek, R. D. Allen, *Science* **218**, 1129 (1982); B. Kachar, D. F. Evans, B. W. Ninham, *J. Coll. Interface Sci.* **99**, 593 (1984).
18. I thank T. S. Reese for continuous support, J. Fex and R. A. Altschuler for providing the specimen of organ of Corti, and J. Handler for providing the A_6 epithelial cells. I also thank J. Zimmemberg, B. Schnapp, P. Bridgman, and B. Andrews for discussions and revision of the manuscript.

24 September 1984; accepted 4 October 1984

Effects of Extracellular Egg Factors on Sperm Guanylate Cyclase

Abstract. *Extracellular factors from the sea urchin egg induce a change in the electrophoretic mobility of an abundant sperm membrane phosphoprotein. The modified protein was identified as guanylate cyclase. The mobility shift of the cyclase was shown to be associated with a decrease in its enzymatic activity.*

Most animal eggs are surrounded by extracellular investments through which sperm pass before contacting the egg surface. These extracellular coats contain molecules that profoundly affect sperm physiology (*1*). The sea urchin egg has a glycoprotein jelly coat that triggers the acrosome reaction (*2*), increased respiration (*3, 4*), and increased motility (*5, 6*) of sperm. The complete sequence of molecular events underlying sperm activation by egg jelly has not been elucidated, although changes in ion flux (*7–10*), membrane potential (*11*), cyclic nucleotide metabolism (*1, 12*), and a number of enzymatic activities (*13–18*) have been described.

We reported earlier that egg jelly induces a change in the electrophoretic mobility of a major membrane protein in *Arbacia punctulata* sperm, from an apparent molecular mass of 160 kilodaltons (kD) to 150 kD (*19*). We now report that the protein is guanylate cyclase, and we show that there is a correlation between the electrophoretic mobility of the protein and its enzymatic activity.

Sea urchin sperm have the highest activity of guanylate cyclase known for any cell (*1*). Isolation of particulate gua-

Fig. 1. Immunoblots showing cross-reaction between polyclonal antiserum to purified *S. purpuratus* sperm guanylate cyclase (*20*) and *A. punctulata* (a) sperm membranes (10 μg), (b) whole sperm (50 μg), and (c) whole jelly-treated sperm (50 μg). The numbers on the left denote apparent molecular mass in kilodaltons. Membranes were prepared as follows: dry *A. punctulata* sperm were diluted (2°C) into 20 volumes of cavitation buffer (480 m*M* NaCl, 10 m*M* $MgCl_2$, 10 m*M* KCl, 5 m*M* adenosine triphosphate, 20 m*M* benzamidine-HCl, 0.5 m*M* phenylmethylsulfonyl fluoride, 10 m*M* MES (*p*H 6.0). The sperm were pelleted (12 minutes at 4000*g*), suspended in 10 volumes of the same buffer, and subjected to nitrogen cavitation (*25*) at 400 pounds per square inch for 10 minutes in a Parr bomb (2°C). The cavitate was centrifuged (2°C) for 10 minutes at 8000*g*, then for 30 minutes at 11,000*g* (discarding the pellet each time). Membranes were pelleted from the second supernatant by centrifugation for 45 minutes at 75,000*g* (2°C). Sperm were treated with egg jelly as described (*19*). Trichloroacetic acid–insoluble protein was prepared and subjected to sodium dodecyl sulfate (Sigma L-5750)–polyacrylamide gel electrophoresis (SDS-PAGE) as described (*19*). Protein was transferred from the gel to nitrocellulose paper in 150 m*M* glycine, 20 m*M* tris (*p*H 8.3), 20 percent (by volume) methanol at 6 V/cm for 14 hours. The nitrocellulose strips were incubated with primary antibody at a dilution of 10^{-3}, and specific antibody binding was visualized by use of a second antibody conjugated with horseradish peroxidase (*26*).